EGT – A sensitive time-of-flight mass spectrometer for multi-element isotope gas analysis

Andreas Riedo[1,2*], Surya Rout[2], Reto Wiesendanger[2], Peter Wurz[2], Ingo Leya[2]

[1]Sackler Laboratory for Astrophysics, Leiden Observatory, Leiden University, The Netherlands
[2]Space Research and Planetary Sciences, Physics Institute, University of Bern, Switzerland

[*]Corresponding Author: riedo@strw.leidenuniv.nl

Abstract: The principles of operation and figures of merit of a novel, compact (324 mm x Ø 114 mm, volume ~1'000 cm^3) reflectron-type time-of-flight mass spectrometer designed for simultaneous multi-element isotope gas analysis is presented. The system, which consists of a pulsed electron impact ion source, is designed either to directly analyse gas samples collected and stored in a compartment or samples extracted from solids using a CW laser system (fiber-coupled diode laser, < 75W, $\lambda = 808 \pm 10$ nm). In latter case, laser pulses are focussed onto the sample surface to spot sizes of ~400 µm in diameter that allows for direct ablation and vaporisation of solid sample material and releasing of trapped gases. A cleaning and trapping system that consists of various cold stages and getters is used before the gas enters the mass analyser. Measurements on various gases were conducted for performance evaluation, ranging from standard gases (Ar, Kr, and Xe) to trapped gases extracted from a sample of the Millbillillie meteorite. At optimised instrument settings, mass spectrometric measurements can be conducted with a mass resolution m/Δm of up to ~1'200 (^{16}O and CH_4 can be resolved), with a dynamic range of ~6 orders of magnitude, and a mass calibration accuracy of ~100 ppm. The high detection sensitivity of the system allows the detection of gas species at partial pressures down to the low 10^{-16} mbar level (corresponding to <10 particles/cm^3 at standard temperature and pressure, including an ion transmission of ~80%). Measurements using standard gases demonstrated that the isotopic ratios for a given element can be measured with an accuracy at the per mill level (relative to terrestrial values). Measurements of Ar extracted from the meteorite Millbillillie gave a $^{36}Ar/^{38}Ar$ ratio of ~1.6, which is in good agreement with literature values.

Keywords: compact time-of-flight mass spectrometer, multi-element isotope analysis, noble gas, sensitive gas analysis, space research

Introduction

Mass spectrometric instruments designed for gas composition analysis (elemental and isotopic) providing a high detection sensitivity coupled with the capability of simultaneous multi-element analysis are of high interest and often mandatory in various fields of scientific research, ranging from, e.g., in situ chemical analysis of planetary atmospheres[1,2] and exospheres[3], analysis of volatile species in the lunar soil[4], composition analysis of volcanic gases[5], to noble gases that are extracted either from meteorites or Earth surface rocks[6,7]. Especially in the field of noble gas (He, Ne, Ar, Kr, Xe) mass spectrometry, instruments having a high detection sensitivity and ionisation efficiency are mandatory as the investigated solid samples are typically highly depleted in these gases. Since the introduction of the concept of measuring in static operational mode, that allows to measure small quantities of a gas (introduced by Reynolds[8], Aldrich and Nier[9] around the 1950's), there is a continuous request for instrumentation with improved figures of merit and measurement capabilities[10-14]. To date, various systems were designed and developed in noble gas mass spectrometry with the goal to improve measurement capabilities, ranging from quadrupole mass spectrometers[15], resonant ionisation mass spectrometers[16-18], mass spectrometer that are coupled to a compressor[12], among others. Sector field mass spectrometers coupled to multi-collector systems are today's state-of-the-art laboratory techniques used in noble gas mass spectrometry as they provide the most accurate isotope ratio analysis[10,19-21]. However, and aside of their undoubted measurement capabilities, these systems are typically designed and optimised for one or a few noble gases and other specific element isotopes only. For the analysis of precious and limited available sample material, such as rare meteoritic samples and extraterrestrial samples from sample-return missions, sensitive and quantitative instrumentation with multi-element isotope analysis capabilities are of interest because such instrumentation allows to address a scientific question from various, complementary sides[17]. This still holds even if such instrumentation do not show the same measurement accuracy on element isotope ratios as the state-of-the-art sector field instrumentation.

In this contribution we present the figures of merit and the measurement capabilities (detection sensitivity, mass resolution and accuracy, ionisation efficiency, and element isotope ratio analysis) of a novel, compact reflectron-type time-of-flight (TOF) mass spectrometer (instrument name EGT,

historically named *E*del*G*as *T*ime-of-flight) designed for sensitive multi-element isotope gas analysis as a complementary instrument to state-of the-art instrumentation. For the characterisation of the instrument performance, measurements were conducted using noble gases from specially prepared standard reservoirs, Ar extracted out of a sample of a meteorite, and using the residual gas within EGT's vacuum chamber.

Experimental

Gas Samples

For the performance characterisation of the EGT, the residual gas within its vacuum chamber (typical base pressure of ~1×10^{-10} mbar, all electronics on), three standard gases (Ar and a mixture of Kr and Xe, all stored in external reservoirs with a total volume of ~1'000 cm^3 and a pipette size of ~1 cm^3 connected to the EGT), and laser extracted Ar from the meteorite Millbillillie[22-24] (~3.5 – 4.0 mg) were analysed. The eucrite meteorite Millbillillie is very well characterized and is generally used as a calibration standard. For the standard gases, a defined volume of Ar (4.12×10^{-7} cm^3STP, corresponding to ~1.1×10^{13} atoms, accuracy ~0.5%) and a mixture of Kr/Xe (Kr: 2.16×10^{-10} cm^3STP, 5.8×10^9 atoms; Xe: 2.21×10^{-10} cm^3STP, 5.9×10^9 atoms; both with an accuracy of ~0.8%) is used for analysis. All three standard gases are of atmospheric isotopic composition[14].

Environment

The experimental setup is located in a temperature controlled laboratory; the nominal temperature and relative humidity is 22±0.5°C and 40±5%, respectively. The dust filtered laminar flow over the entire surface area does not only guarantee stable conditions for the operation of the instrument it also allows proper sample handling, i.e., sample preparation and loading the sample into the laser extraction unit.

Experimental Setup and Principles of Operation of the EGT

The multi-element isotope gas analyser is a compact (324 mm × ∅ 114 mm, volume ~1'000 cm^3) reflectron-type time-of-flight mass spectrometer. The design is based on extensive ion trajectory simulations using the software SIMION (Scientific Instrument Services, Inc., USA) and the instrument was built in-house to utmost UHV standards.

Figure 1 shows the schematics and principles of operation of the instrument. The system has five gate valves, including two towards the pumping system, one for the gas inlet, and one for a cold trap containing activated charcoal for freezing Ar and CO_2 during He-Ne measurements because both gases would produce double charged interferences on ^{20}Ne and ^{22}Ne, respectively. The fifth gate valve connects the spectrometer to a metal getter (SAES®) to reduce the H_2 background in the spectrometer because high H_2 amounts would naturally result in high ^1H-^2H amounts, which interferes with the ^3He signals. The pumping system connected to the EGT consists of an ion getter pump (IG1) and a turbomolecular pump (TMP1). The latter is pumping to a reservoir (RES1), which is evacuated from time to time (if $p > 10^{-2}$ mbar) by a turbomolecular pump, which is connected to a four-chamber membrane pump (RVTMP). Because the system is designed for low gas amounts, the EGT is not actively pumped during measurements (static mode)[8,12]. After a measurement the remaining gas is evacuated by TMP1 to prevent contamination of IG1. The gate valve to IG1 is only opened if the system is in standby mode. In standby mode the valve to TMP1

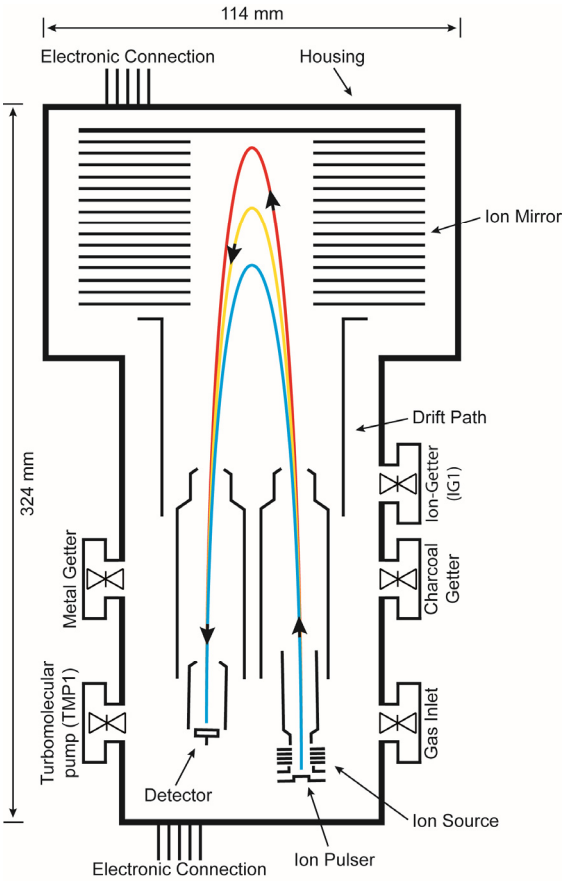

Fig. 1 Schematic drawing and principles of operation of the EGT. The gas enters the instrument through the gas inlet valve. At the electron impact ion source the gas is ionised and pulsed into the mass analyser after passing through the ion source optics. After passing the field free drift path the ions are reflected at the ion mirror towards the detector system and passing a second time the drift path.

is closed to prevent venting the system in case of a pump breakdown. The gate valve for gas inlet is connected to a cross made of standard vacuum components, which is connected to the reservoirs of the standard gases and to a laser ablation setup, which allows gas extraction from solid silicate materials (discussed later). The cross is evacuated by a second turbomolecular pump (TMP2), which is also pumped into a reservoir (RES2). This reservoir is connected to the same pump system (turbomolecular pump and RVTMP) as the reservoir of the EGT. Once the sample gas is introduced into the cross piece, the gate valve of the gas inlet is opened for five minutes to guarantee pressure equilibration. After the five minutes the gate valve is closed and the remaining gas in the cross piece is pumped (TMP2).

A pulsed and emission controlled electron-impact source is used for ionisation of the gas species. In the current design, we use a commercial Lanthanum-Hexaboride (LaB_6) single crystal as an electron emitter, which is mounted on a carbon wire (Kimball Physics Inc., USA) and operated and kept at a constant emission current of 250 µA. To ensure optimal working conditions, i.e., a stable temperature and no risk of contamination, the filament is always operated at a constant emission current. Once the gas is ionised, the ions are pulsed into the ion optics of the system. The repetition frequency of the pulser can be adjusted (≤ 10 kHz, rise time ~4.6 ns) for optimal measurement conditions. Note that the lower the pulse frequency the more ions can be stored in the ion source[25]. However, a longer storage time of the ions in the source region can also result in unwanted non-linear effects, i.e., detector saturation, sensitivities or fractionation factors that depend on the gas amounts. First, the ions pass the ion optics for acceleration, focussing, and confinement before entering the field free drift region for mass separation. At the gird-less ion mirror, the ionised species are reflected towards the detector system and finally they pass a second drift path. The ions sequentially arrive at the detector system, according to their mass over charge ratio (time-of-flight measurement principle). The in-house designed detector system consists of multichannel-plates (MCP, chevron configuration, quality diameter of 8 mm) for the generation of electric signals and an anode of Apollonius design for collecting the generated electron avalanches[26,27]. A high-speed analogue-to-digital converter (ADC) card (2 channels, max. sampling rate of 3.2 GS/s, 12 bit, U5303A, Acqiris, Switzerland; former Keysight and Agilent) is used for recording TOF spectra on the host computer. An in-house designed software is used for data analysis, including conversion between TOF to mass spectra, integration of signals, accumulation of TOF spectra, among others. A detailed description of the software can be found in one of our previous publications[28].

Laser ablation extraction system

The laser extraction line is designed for the extraction and cleaning of small amounts of gas from solid, mostly silicate materials. The line can be divided in two main parts, i) the laser extraction part and ii) a gas cleaning part. The entire line is evacuated using a turbomolecular pump (TMP3) connected to a reservoir (RES3) which is again from time to time (if $p > 10^{-2}$ mbar) evacuated using the turbomolecular pump/RVTMP system (see also above). The extraction laser is a CW fiber-coupled diode laser (<75 W, λ=808±10 nm). The output power can be controlled remotely to optimise ablation or melting of the sample. The laser system is positioned outside the vacuum setup and the laser beam is pointed towards the sample with a beam diameter of ~400 µm. A red guidance pilot laser helps in targetting and navigating the laser on the sample. The sample and the laser ablation is viewed in realtime using an attached video camera. The temperature achieved during the laser ablation is measured using a well calibrated two color pyrometer. Samples are placed in cavities on a custom-built sample holder, which is installed in an all metal vacuum chamber except for the viewport on top, just below the laser. In Fig. 2 a region of the powdered Millbillillie meteorite is shown before and after laser ablation. After laser melting at ~2000°C the silicate minerals transform into a glassy form due to the rapid cooling, which is a clear indication for melting the sample.

The gas extracted during laser ablation passes first through a U-shaped stainless-steel carrier line that is

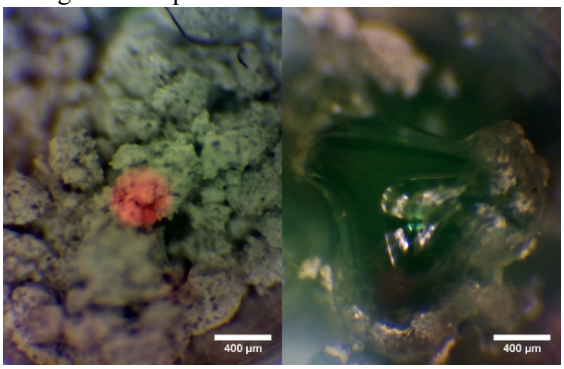

Fig. 2 Real-time imaging of the sample allows to optimise laser ablation and evaporation of sample material. Left: The pilot laser spot in red (400 µm in diameter) is used for targeting the raw material (here a sample of the meteorite Millbillillie). Right: Sample material after laser ablation.

cooled with liquid nitrogen to freeze-out water. Adsorbed water is abundant in the investigated powdered Millbillillie meteorite and also typically in

other silicate mineral samples. Next, the gases cleaned of water passes through a cross piece at which two metal getters (SAES®) and two cold traps filled with activated charcoal are connected. At the working temperature of 280°C the getters efficiently clean the gas from nitrogen and hydrocarbons. The two activated charcoals can be cooled to temperatures in the range of either -100°C to -135°C or -196°C for selective trapping of Kr-Xe and Ar, respectively. During the studies presented here, none of the cold traps were used. After laser melting we wait 10 min for gettering and gas equilibration before the gas is introduced into the cross piece that is directly connected to the EGT (see above).

Measurements

A typical measurement run consists of *i*) a measurement of the background of the EGT in static operational mode, and *ii*) a measurement of the sample gas. The background signals are subsequently subtracted from the signals of the sample gas. For calibration purposes, standard gases can be measured before and after the measurements. Between each measurement, all the vacuum compartments are evacuated to the typical base pressures. During a typical measurement run, several 10'000 to 100'000 TOF spectra are recorded. Similar to studies using another setup[29,30], the spectra are accumulated on board the ADC card to several thousand before saving the accumulated spectra on the host computer. This procedure allows real-time monitoring of the measurement stability during a measurement campaign.

Instrumental Performance and Discussion

Sensitivity

Figure 3 depicts a measurement of the residual gas within the EGT (p_{tot} = 1.1×10^{-10} mbar, gate to TMP1 open, gate to IG1 closed). The measurement consists an accumulation of 10^6 TOF spectra in total (500 accumulated files, each consists of 2'000 spectra). For the conversion of recorded signals to partial pressures, we assume that the pressure measured by the cold-cathode gauge that is directly connected to the EGT is given by the four major peaks in the mass spectrum, i.e., H_2, H_2O, CO, and CO_2. The left panel of Fig. 3 shows an overview spectrum of the mass range (m/z) 1 to ~230. Interestingly, the isotopes of Hg with a maximum partial pressure of 10^{-14} mbar can easily be observed (^{202}Hg with ~500 particles/cm^{3}STP). Currently, the source of the Hg is unknown as only certified materials without any known Hg impurities were used for construction. However, the detected partial pressure of Hg is very low and even a minor contamination during manufacturing could be the reason. Such a contamination could be, e.g., by using tools that were in contact with, e.g., soldering wires, which are known to contain trace abundances of Hg. Interestingly, the amount of the Hg contamination could not be reduced even after several bake-outs of the vacuum system (~200°C for several days); the signal stayed constant. On the right panel of Fig. 3 the mass range ~165 to ~185 is shown in more detail. It can be seen that ion species with partial pressures >3×10^{-16} mbar can be detected. With an ion transmission of ~80% (derived from SIMION simulations) less than ~10 particles/cm^{3}STP can be

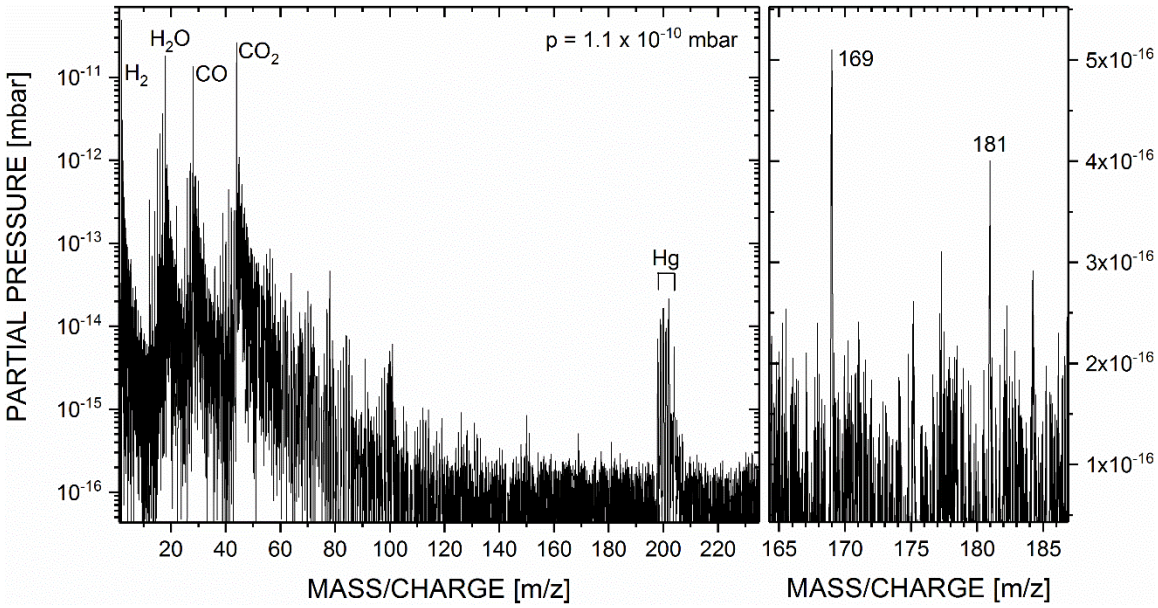

Fig. 3 Measurement of the residual gas in the EGT. The total pressure as measured with a cold-cathode gauge was ~1.1×10^{-10} mbar. The detection sensitivity of the instrument allows measuring partial pressures down to the lower 10^{-16} mbar level.

detected in an integration time of ~1'850 seconds. The sufficiently high mass resolution and accuracy of the mass scale calibration (discussed later) allows distinguishing between "real" mass peaks and electronic or captured noise peaks. Real peaks only appear at full numbers (at least close to, given the actual mass and assuming only single charged ions); a peak appearing between two entire (m/z) values would be considered as a noise peak.

The measurement of the residual gas allows furthermore to define the dynamic range of the system (left panel of Fig. 3). The simultaneous measurement of gas species with partial pressures in the range from high 10^{-11} mbar to low 10^{-16} mbar points to a dynamic range of about 6 orders of magnitude.

Mass Resolution

Figure 4 shows the mass resolving power m/Δm of the EGT as a function of the mass over charge ratios (m/z) of the detected ion species. We used the mass spectrum shown in Fig. 3 for the mass calibration. At low (m/z) values, ranging from H to about O, the mass resolution increases with increasing (m/z) up to a value of ~800. This trend is limited due to electronic interferences with the pulser, which has a rise time of ~ 4.6 ns (see red dashed line). After the steep trend the mass resolution still increases with increasing (m/z) to values of ~1'200, though the slope is shallower.

A mass resolution of ~800 achieved already at (m/z) values lower than ~20 allows the simultaneous detection and identification of ^{16}O and CH_4 (see top panel of Fig. 5). Depending on the scientific question, this performance could be of interest as the abundance of both peaks can in principle be quantified using a multi peak fit function. At (m/z) values of single charged Hg, a mass resolution of ~1'200 is reached (see bottom panel in Fig. 5). Remarkably, the detected Hg isotope peaks with a partial pressure of ~8×10^{-14} mbar and lower (see also Fig. 3) are all sufficiently separated, which allows reliable isotope ratio analyses (see discussion in Section *Isotope Measurement Accuracy*).

Detector System – Single ion event measurements

The detector system consists of two MCP plates (chevron configuration, Photonis USA, Inc., USA) for detecting the ions and generating electron avalanches, and an anode of Apollonius design, both designed in-house. The MCPs used in this configuration have a quality diameter of 8 mm, a pore diameter of 10 µm, a pitch of 12 µm, a bias angle of 8°, and an L/D ratio of 60:1.

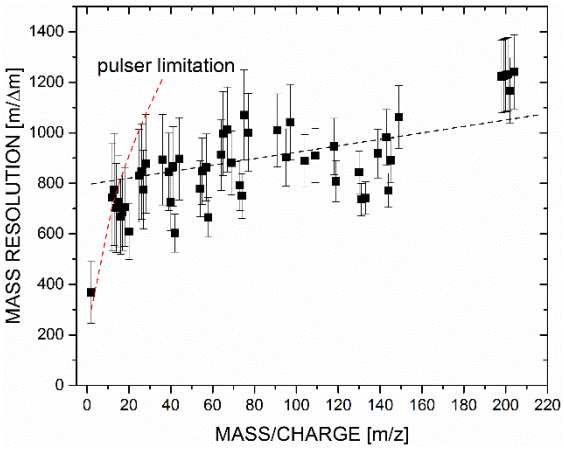

Fig. 4 Mass resolution m/Δm of the EGT as a function of the mass/charge (m/z) ratio. In the mass range below ~16, the mass resolution is limited by electronic interferences with the pulser (dashed line in red). After the rise-time of the pulser the full mass resolution of up to 1'200 can be reached.

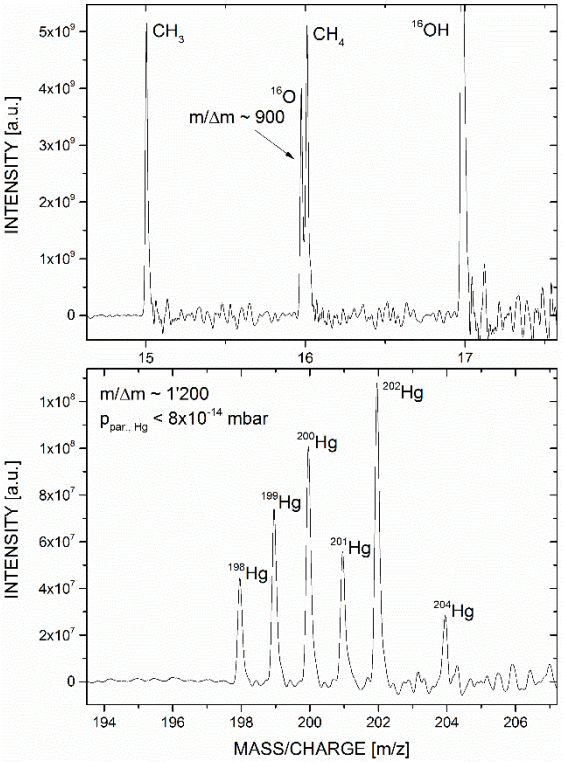

Fig. 5 Parts of a mass spectrum showing the signals in the mass range around ^{16}O (top panel) and Hg (bottom panel). The steep increase of the mass resolution m/Δm (see Fig. 4) allows to separately detect ^{16}O and CH_4. At high mass/charge ratios the Hg isotopes can be detected with a mass resolution of ~1'200.

For the performance characterisation of the detector system, including speed and signal amplification of incoming ions, single ion event measurements were performed at different gain levels, with a similar procedure as discussed in ref. 31. MCP operating voltages in the range of ΔV = 1700 – 2000 V were applied to the MCP stack (ΔV = voltage front MCP – voltage back MCP). The voltage was increased stepwise by 50 V. During measurements, the voltage

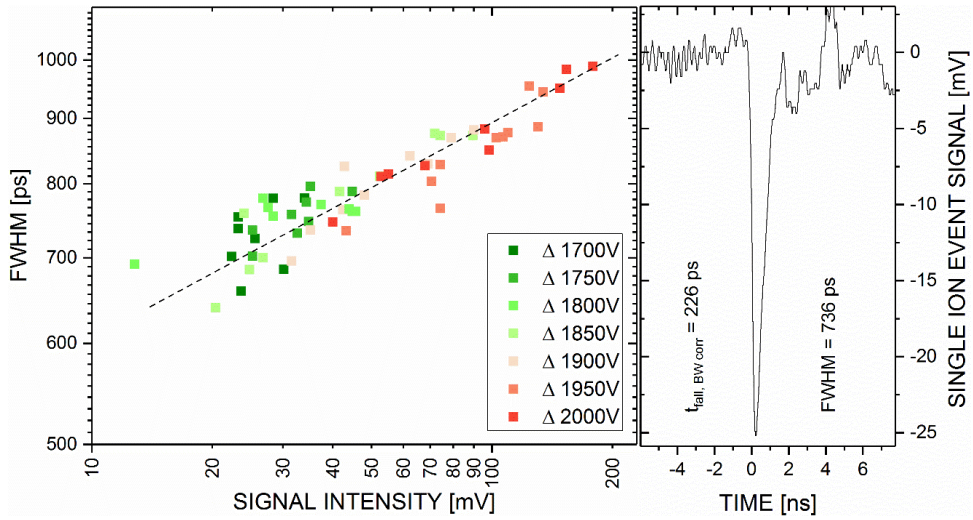

Fig. 6 Left: Correlation between detected signal amplitudes and pulse widths (FWHM) of single ion events at various applied potential differences ΔV over the MCP stack in the range of 1.7 – 2.0 kV. Right: Detected signal of an ion single event. A FWHM of 736 ps and a bandwidth corrected fall time (10% to 90% level) of 226 ps was measured at a peak amplitude of about 25 mV.

at the back of the MCPs was kept constant at –300 V, which give the best electronic connection between the back of the MCP stack and the Apollonius anode. At each MCP operating voltage 4 – 10 individual measurements were conducted. A digital phosphor oscilloscope (DPO) with a high sampling rate and a high bandwidth was used for single ion event detection (Tektronix, DPO 7354c, 40 GS/s, 3.5 GHz BW). Therefore, the DPO offered a higher sampling rate and a larger BW than the ADC card typically used. For the measurement of single ion signals only the detector system was switched on (ion optics and ion source were switched off), and the system was pumped actively by its TMP1, i.e., the gate valve to IG1 was closed. The base pressure during the measurements was ~1.9×10^{-11} mbar. Positively charged ions that were either produced in interactions of cosmic rays and/or from the cold cathode gauge connected to the ETG were used for this measurement.

The left panel of Fig. 6 displays the correlation between signal intensities and the full width measured at half maximum (FWHM) of detected single ion events. It can be seen that the FWHM increases with increasing signal intensities. At the lowest signal intensity a FWHM of ~650 ps was measured; the value reaches ~1 ns at the highest intensities. In addition, the expected trend of increasing signal intensities with increasing operating voltage is also visible (see colour coded symbols). At an MCP operating voltage of ΔV = 2 kV a large signal of ~200 mV is recorded for a single ion detection. On the right panel of Fig. 6 a measurement of a single ion event recorded with ΔV = 1700 V is shown. The peak with an amplitude of about 25 mV is very symmetric with a FWHM of 736 ps and a fast falling time of 226 ps (bandwidth (BW) corrected)[27,31].

In comparison to our previous publication, in which we discussed an MCP detector system coupled to a segmented anode of microstrip design (FWHM down to 250 ps and falling times down to ~170 ps, BW corrected)[32], the system discussed in this contribution shows larger FWHMs and slightly increased fall times. However, the efficient electron capture of the Apollonius anode, which is more than two times higher than in the previous study, is one of the reasons why the EGT has a high detection sensitivity down to the 10^{-16} mbar level. Furthermore, the observed increased FWHM is not compromising the instrument performance because the FWHM is currently not limiting the observed mass resolving power of the EGT. However, the FWHM could easily be improved (rising edge) and is planed in the future by, e.g., adding capacitors near the detector system, allowing for a fast recharging of the MCP's[32]. Currently, the integration of electric components inside the EGT is kept at minimum to guarantee very low outgassing and therefore low base pressures, which is required for reliable measurements of very low gas amounts.

Ionisation Efficiency

The ionisation efficiency of the EGT can be characterised by studying if and by how much the signal of the gas species of interest is decreasing. Figure 7 depicts the ^{40}Ar signal (calibration gas) as a function of the measurement time. In this measurement campaign more than 2'500 accumulated spectra were recorded and saved on the host computer, each consisting of 2'000 single spectra (giving 5×10^{6} recorded spectra in total); the

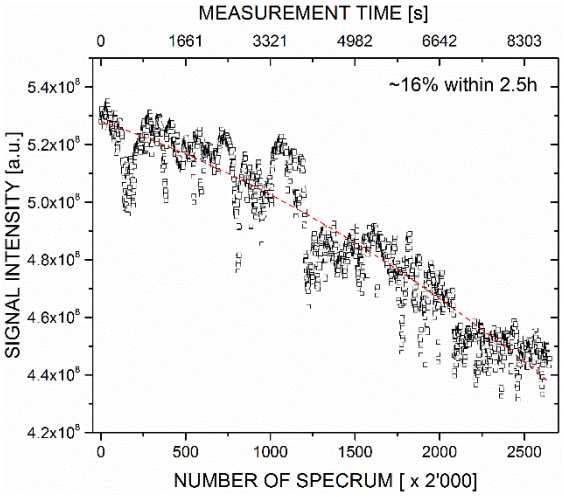

Fig. 7 Intensity of the ^{40}Ar signal as a function of measurement time. In ~2.5 hours ~16% of the gas is ionised and measured.

acquisition lasted 8804 s (about 2 h and 27 minutes). Within this measurement period the ^{40}Ar signal decreases by ~16%. Physically, the decrease must be exponential. However, for small gas usages, the exponential behaviour can well be approximated using a linear relationship. For comparison, the decrease of ^{40}Ar in a sector field mass spectrometer (MAP 215-50, 90°, 15 cm radius) routinely used in our laboratory is 90% in 2.5 hours. This slow signal decrease, in comparison to the MAP instrument, is of high interest as the measurement accuracy increase with the increase of measurement time, corresponding to an increase of number of recorded spectra (see following section *Isotope Ratio Measurement Accuracy*).

Mass Calibration Accuracy

For the conversion between TOF and mass spectra we use a quadratic equation of the type $(m/z)_i(t) = k_0(t_i-t_0)^2$, where *i* is an index of an identified peak of an isotope or molecule and k_0 and t_0 are fit-parameters of the linear regression used for the calibration. For the characterisation of the mass calibration accuracy a mixture of Ar and Kr/Xe standard gases was measured. The left panel in Fig. 8 displays the linear regression between the time-of-flight of identified species and the square-root of their mass to charge ratios. Since sufficient mass peaks were available, only singly charged species are used for calibration. The middle panel of Fig. 8 depicts the mass residuals of ionised species used for calibration (the x-axis denotes the ith identified isotope/molecule peak). The residuals are defined as ($Mass_{Calc}$ – $Mass_{Lit}$) where $Mass_{Calc}$ denotes the calculated mass of the identified isotope/molecule using the fit constants t_0 and k_0 and $Mass_{Lit}$ the literature mass. Remember that heavier ionised species arrive later at the detector system. The right panel of Fig. 8 shows a histogram of the mass residuals. There is Gaussian distribution and 50% of detected and identified peaks are within a mass calibration accuracy of about ±100 ppm; about 87% of the peaks used for mass calibration have an accuracy of about ±300 ppm or better. Note that the result is in good agreement with the estimation that the mass calibration accuracy should be about ten times larger than the instrumental mass resolving power (calibration accuracy ~ 1/(10 times mass resolution)). The EGT has a mass resolution (m/Δm) in the range 800 - 1'200 (see Figs. 4 and 5), which corresponds to an accuracy in the mass scale of ~100 ppm.

Isotope Ratio Measurement Accuracy

For the characterisation of the isotope ratio measurement accuracy of the EGT we measured *i*) the noble gases Kr and Xe from our calibration standards, *ii*) Hg within the background of the EGT, and *iii*) Ar laser extracted from a sample of the Millbillillie meteorite. The accuracy is defined as ($IsoAbund_{Lit}$ – $IsoAbund_{Meas}$) / $IsoAbund_{Lit}$, where $IsoAbund_{Lit}$ denotes the literature value of the isotope abundance and $IsoAbund_{Meas}$ the measured isotope abundance. For the Kr and Xe standard gas

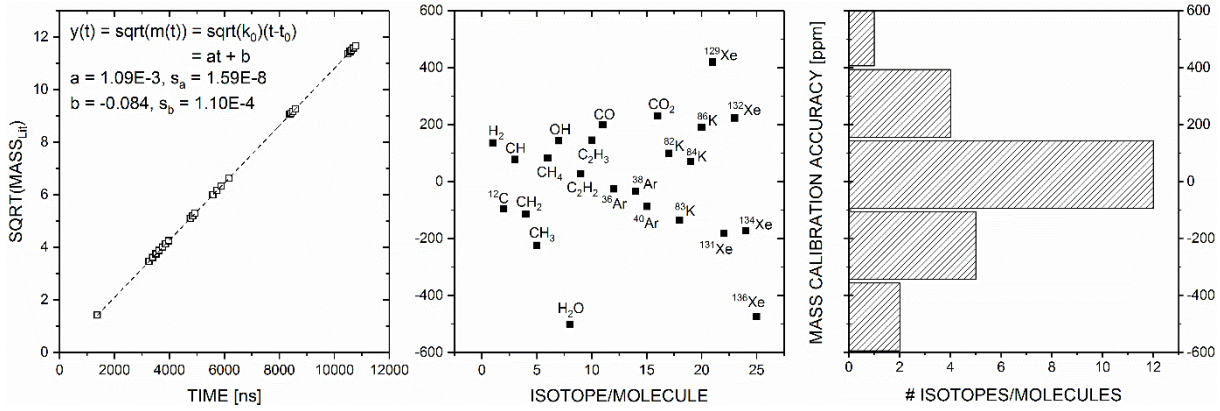

Fig. 8 Mass calibration accuracy of the EGT. A linear regression of the square-root of the mass as a function of the time-of-flight determines the fit parameter needed for mass calibration (left panel). Residuals of the mass calibration are shown in the middle panel which are also shown as a histogram (right panel). The accuracy of the mass calibration is in the range ± 100 ppm.

measurements and for the measurements of Ar from Millbillillie, the background signals were subtracted. In total 10^6 spectra were recorded in each measurement, accumulated in 1'000 files, each consisting 1'000 single spectra. For the Hg background measurement, 2'000 files, each consisting 1'000 spectra were recorded. For all three types of measurements the number of recorded spectra could easily be increased because for Kr and Xe the decrease of signal intensity over time is only moderate and the background of Hg is very stable. With the increase of measurement time, and hence the number of recorded spectra the measurement accuracy can be increased with square root of recorded spectra. This is true until other factors dominate the measurement accuracy, such as electronic noise from the measurement card, background of residual gas or accuracy of peak integration.

Figure 9 depicts recorded mass spectra (left panel) and the accuracy of the isotope ratios (right panel). For calculating the latter we assume terrestrial values for Hg[33] and we used the isotopic composition of the terrestrial atmosphere for Kr and Xe[14]. All Kr isotopes could be detected during the measurement (Kr partial pressure $<8.8\times10^{-13}$ mbar). Krypton-78, which has the lowest abundance of all Kr isotopes with a partial pressure of $\sim3\times10^{-15}$ mbar, is slightly affected by the background noise (see insert) and is therefore not considered for isotope ratio analysis. The isotope ratios were measured with an accuracy of better than ~3%; the major isotope ^{84}Kr was measured with an accuracy of better than 7‰. The result is slightly better for Xe isotopes. All Xe isotopes (Xe partial pressure of $<2.2\times10^{-13}$ mbar) were detected and identified; even the Xe isotopes with the lowest abundance, ^{124}Xe and ^{126}Xe (at partial pressures of $\sim2\times10^{-16}$ mbar). Since the peaks of ^{124}Xe and ^{126}Xe are affected by the baseline noise

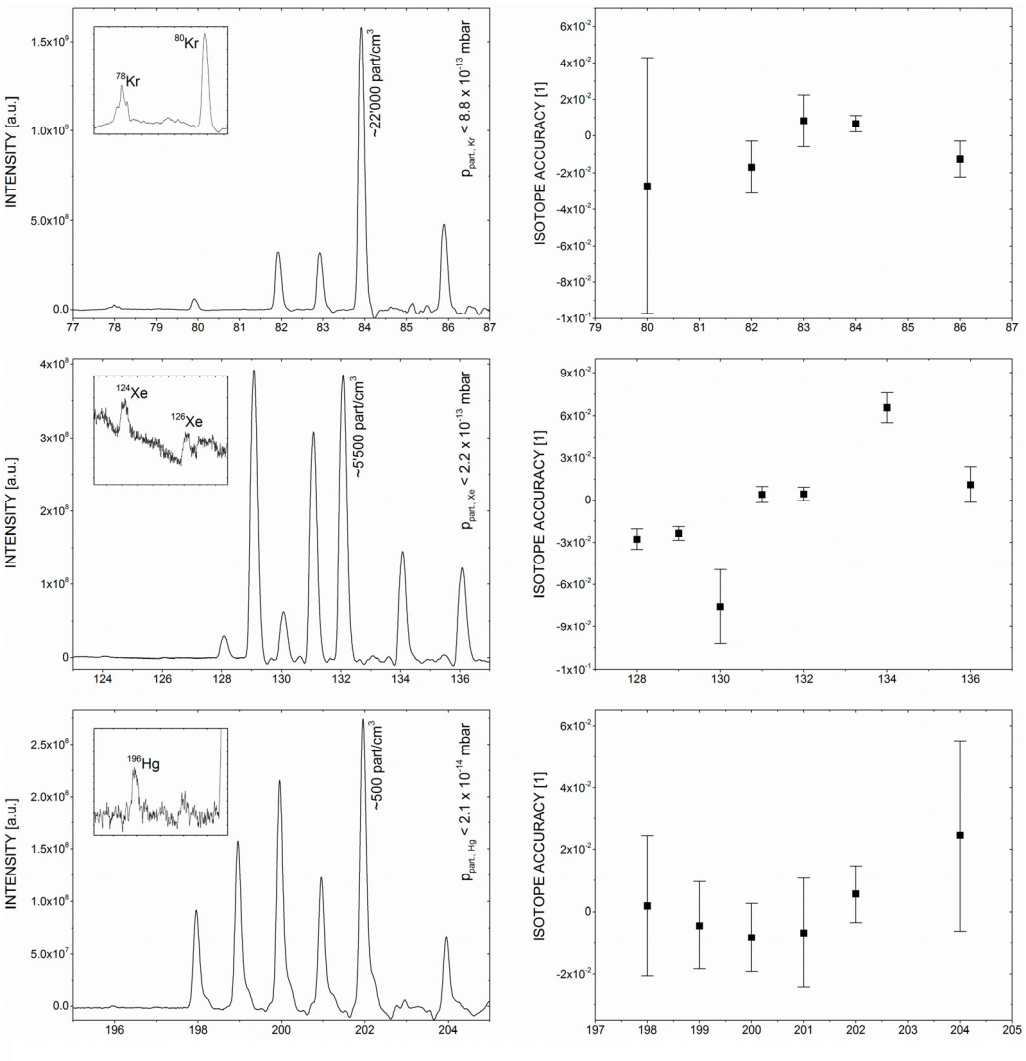

Fig. 9 Mass spectra of Kr, Xe, and Hg isotopes (left row). Accuracy of isotope ratio analysis for the detected elements (right row). Best isotopic accuracy are typically observed for the major isotopes. Overall best accuracies are observed for Hg. See text for more information.

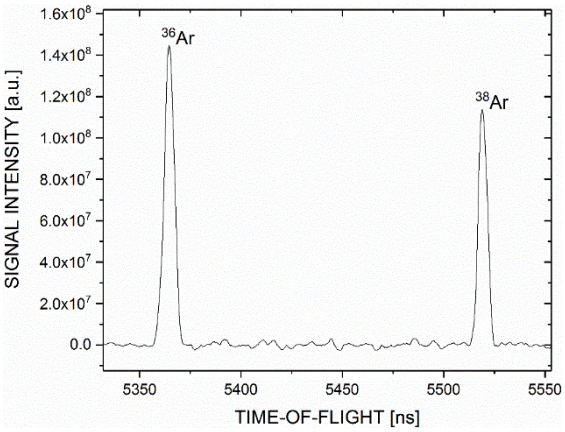

Fig. 10 Argon measurement of the Millbillilie meteorite. Shown are ^{36}Ar and ^{38}Ar signals. The shown spectra is after blank correction.

(see insert), they were both not considered for isotope ratio analysis. For the majority of the isotopes, an accuracy of better than ~3% is reached; the major isotopes ^{131}Xe and ^{132}Xe can be measured with an accuracy of ~4‰.

All Hg isotopes could be detected with partial pressures $<2.1\times10^{-14}$ mbar. However, for the lowest abundant isotope ^{196}Hg (partial pressure $\sim3\times10^{-16}$ mbar) the signal-to-noise ratio is very low (see insert); this isotope is therefore not considered for the ratio analysis. For ^{204}Hg, which is second lowest in abundance, an accuracy of ~2.4% was measured. All other isotopes of Hg were detected with an accuracy at the per mill level. At a first glance, it is surprising that Hg, which has the lowest partial pressure among all studied elements in this study, can be measured with the highest accuracy. The unexpected result is due to the background in the EGT (see Fig. 3). There is a significant background at (m/z) values below ~150, which increases towards smaller (m/z) values and reaches a maximum at the level of (m/z) ~ 50. For Kr and Xe measurements the background is significant and its subtraction compromises the accuracy of isotope ratio measurements. Consequently, reducing the background at lower (m/z) values will significantly increase the accuracy of the isotope ratio measurements for all noble gas species.

Figure 10 depicts the results of the Ar measurement for the Millbillillie meteorite. Remember that we selected powders from the bulk meteorite and fully degassed this sample. Therefore, we cannot expect any spatial information concerning sampling depth and/or individual minerals or spots in the sample. All gas extracted during melting was collected and measured. The relevant isotopes ^{36}Ar and ^{38}Ar were clearly detected and - as expected - their abundance significantly deviates from terrestrial values. Using results obtained earlier by us on the same meteorite but using sector field mass spectrometry we can calculate that in this experiment we have extracted ~10^9 atoms of ^{36}Ar from the ~3.5 mg of Millbillilie. For the extracted gas, we measured a ^{36}Ar/^{38}Ar ratio of ~1.6, which is well within the range of literature values (0.7 – 5.2)[23,24,34].

Conclusions

In this contribution, we present the measurement capabilities and figures of merit of a novel, compact reflectron-type time-of-flight mass spectrometer for multi-element isotope gas analysis. Measurements were conducted on Ar, Kr, and Xe standard gases, background gas within the instruments vacuum chamber showing trace amounts of Hg, and Ar extracted from the meteorite Millbillillie using a laser ablation setup.

The measurements demonstrate that the instrument has a dynamic range of about six orders of magnitude, a mass resolving power (m/Δm) of up to ~1'200 (measured at Hg, ^{16}O and CH_4 can be separated), and a high detection sensitivity, which allows the detection and identification of species at a partial pressure down to the low 10^{-16} mbar level. Single ion measurements showed that the in-house designed and built detector system (MCPs in synergy with an Apollonius anode) generates electric signals ranging from 20 mV to 200 mV per single ion event, corresponding to measured FWHM of detected peaks ranging from ~650 ps to ~1 ns, respectively. Measurements of single ion events showed fall times (bandwidth corrected) of better than 250 ps. The rise-time could be shortened and the FWHM improved by integrating capacitors near the detection system.

Our isotope ratio measurements demonstrate that an accuracy at the per mill level can be reached. The best accuracy is reached for Hg, which is a contaminant and which has a partial pressure of $<2.1\times10^{-14}$ mbar. The minor isotopes of Kr and Xe were measured at the 2-3% level or better. The slightly lower accuracy at lower (m/z) values is due to the background correction; the background significantly increases towards lower (m/z) values. Consequently, an improvement of the background at lower (m/z) values will significantly improve the accuracy of the isotope ratio measurements of the noble gases. Measurements of Ar extracted from the meteorite Millbillillie gave a ^{36}Ar/^{38}Ar ratio of ~1.6, which agrees with literature values.

In summary, the EGT is a compact and sensitive multi-element isotope gas analyser. The measurement performance of the EGT allows its

operation in various scientific disciplines, ranging, e.g., from the analysis of atmospheric gases to gases extracted from various types of solids. Especially in case limited and precious sample material is available only, the current figures of merit are of high interest as the system can provide the chemical composition (element and isotopes) in a global context manner.

Acknowledgements

This work is supported by the Swiss National Science Foundation.

References

[1] P.R. Mahaffy, H.B. Niemann, A. Alpert, S.K. Atreya, J. Demick, T.M. Donahue, D.N. Harpold, T.C. Owen. Noble gas abundance and isotope ratios in the atmosphere of Jupiter from the Galileo Probe Mass Spectrometer. *J Geophys Res-Planet.* **2000**, *105*(E6), 15061.

[2] D. Abplanalp, P. Wurz, L. Huber, I. Leya, E. Kopp, U. Rohner, M. Wieser, L. Kalla, S. Barabash. A neutral gas mass spectrometer to measure the chemical composition of the stratosphere. *Advances in Space Research.* **2009**, *44*(7), 870.

[3] S. Meyer, M. Tulej, P. Wurz. Mass spectrometry of planetary exospheres at high relative velocity: direct comparison of open- and closed-source measurements. *Geosci Instrum Method Data Syst.* **2017**, *6*(1), 1.

[4] L. Hofer, P. Wurz, A. Buch, M. Cabane, P. Coll, D. Coscia, M. Gerasimov, D. Lasi, A. Sapgir, C. Szopa, M. Tulej. Prototype of the gas chromatograph–mass spectrometer to investigate volatile species in the lunar soil for the Luna-Resurs mission. *Planetary and Space Science.* **2015**, *111*, 126.

[5] F. Sortino, A. Nonell, J.P. Toutain, M. Munoz, M. Valladon, G. Volpicelli. A new method for sampling fumarolic gases: Analysis of major, minor and metallic trace elements with ammonia solutions. *Journal of Volcanology and Geothermal Research.* **2006**, *158*(3), 244.

[6] P.C. Stephenson, Y. Lin, I. Leya. The noble gas concentrations of the Martian meteorites GRV 99027 and paired NWA 7906/NWA 7907. *Meteoritics & Planetary Science.* **2017**, *52*(12), 2505.

[7] R. Wieler, L. Huber, H. Busemann, S. Seiler, I. Leya, C. Maden, J. Masarik, M.M.M. Meier, K. Nagao, R. Trappitsch, A.J. Irving. Noble gases in 18 Martian meteorites and angrite Northwest Africa 7812—Exposure ages, trapped gases, and a re-evaluation of the evidence for solar cosmic ray-produced neon in shergottites and other achondrites. *Meteoritics & Planetary Science.* **2016**, *51*(2), 407.

[8] J.H. Reynolds. High Sensitivity Mass Spectrometer for Noble Gas Analysis. *Review of Scientific Instruments.* **1956**, *27*(11), 928.

[9] L.T. Aldrich, A.O. Nier. Argon 40 in Potassium Minerals. *Physical Review.* **1948**, *74*(8), 876.

[10] P.G. Burnard, R. Basset, M. Pujol, B. Marty. High resolution, multicollector noble gas mass spectrometry: HELIX-MC. *Geochimica et Cosmochimica Acta.* **2006**, *70*(18, Supplement), A75.

[11] C.M. Hohenberg. Noble gas mass spectrometry in the 21st century. *Geochimica et Cosmochimica Acta.* **2006**, *70*(18, Supplement), A258.

[12] T. Matsumoto, J. Matsuda, I. Yatsevich, M. Ozima. Noble gas mass spectrometry with a compressor driven recycling system for improved sensitivity. *Geochem J.* **2010**, *44*(3), 167.

[13] C.M. Hohenberg. High sensitivity pulse-counting mass spectrometer system for noble gas analysis. *Review of Scientific Instruments.* **1980**, *51*(8), 1075.

[14] D. Porcelli, C.J. Ballentine, R. Wieler. An overview of noble gas - Geochemistry and cosmochemistry. *Rev Mineral Geochem.* **2002**, *47*(1), 1.

[15] Y. Aregbe, S. Valkiers, K. Mayer, P. De Bièvre. Comparative isotopic measurements on xenon and krypton. *International Journal of Mass Spectrometry and Ion Processes.* **1996**, *153*(1), L1.

[16] E. Gilabert, B. Lavielle, B. Thomas, S. Topin, F. Pointurier, C. Moulin. Ultratrace analysis of krypton isotopes by resonant ionization spectroscopy-time of flight mass spectrometry (RIS-TOF). *Journal of Analytical Atomic Spectrometry.* **2016**, *31*(4), 994.

[17] I. Strashnov, D.J. Blagburn, J.D. Gilmour. A resonance ionization time of flight mass spectrometer with a cryogenic sample concentrator for isotopic analysis of krypton from extraterrestrial samples. *Journal of Analytical Atomic Spectrometry.* **2011**, *26*(9), 1763.

[18] J.D. Gilmour, I.C. Lyon, W.A. Johnston, G. Turner. RELAX: An ultrasensitive, resonance ionization mass spectrometer for xenon. *Review of Scientific Instruments.* **1994**, *65*(3), 617.

[19] V.S. Heber, R.C. Wiens, A.J.G. Jurewicz, N. Vogel, D.B. Reisenfeld, H. Baur, K.D. McKeegan, R. Wieler, D.S. Burnett. Isotopic and elemental fractionation of solar wind implanted in the Genesis concentrator target characterized and quantified by noble gases. *Meteoritics & Planetary Science.* **2011**, *46*(4), 493.

[20] R. Wieler. 15.19 - Noble Gas Mass Spectrometry A2 - Holland, Heinrich D. In: Turekian KK, ed. *Treatise on Geochemistry (Second Edition).* Oxford: Elsevier; 2014:355.

[21] T.R. Ireland. Invited Review Article: Recent developments in isotope-ratio mass spectrometry for geochemistry and cosmochemistry. *Review of Scientific Instruments.* **2013**, *84*(1), 011101.

[22] A. Yamaguchi, H. Takeda, D.D. Bogard, D. Garrison. Textural variations and impact history of the Millbillillie eucrite. *Meteoritics.* **1994**, *29*(2), 237.

[23] O. Eugster, T. Michel. Common asteroid break-up events of eucrites, diogenites, and howardites and cosmic-ray production rates for noble gases in achondrites. *Geochimica et Cosmochimica Acta.* **1995**, *59*(1), 177.

[24] H. Busemann, O. Eugster. The trapped noble gas component in achondrites. *Meteoritics & Planetary Science.* **2002**, *37*(12), 1865.

[25] D. Abplnalp, P. Wurz, L. Huber, I. Leya. An Optimised Compact Electron Impact Ion Source for a time-of-flight mass spectrometer. *International Journal of Mass Spectrometry.* **2010**, *294*, 33.

[26] P. Wurz, L. Gubler. Impedance-matching anode for fast timing signals. *Review of Scientific Instruments.* **1994**, *65*(4), 871.

[27] P. Wurz, L. Gubler. Fast microchannel plate detector for particles. *Review of Scientific Instruments.* **1996**, *67*(5), 1790.

[28] S. Meyer, A. Riedo, M.B. Neuland, M. Tulej, P. Wurz. Fully automatic and precise data analysis developed for time-of-flight mass spectrometry. *Journal of Mass Spectrometry.* **2017**, *52*(9), 580.

[29] A. Riedo, A. Bieler, M. Neuland, M. Tulej, P. Wurz. Performance evaluation of a miniature laser ablation time-of-flight mass spectrometer designed for in situ investigations in planetary space research. *Journal of Mass Spectrometry.* **2013**, *48*(1), 1.

[30] A. Riedo, S. Meyer, B. Heredia, M.B. Neuland, A. Bieler, M. Tulej, I. Leya, M. Iakovleva, K. Mezger, P. Wurz. Highly accurate isotope composition measurements by a miniature laser ablation mass spectrometer designed for in situ investigations on planetary surfaces. *Planetary and Space Science.* **2013**, *87*, 1.

[31] R. Schletti, P. Wurz, S. Scherer, O.H. Siegmund. Fast microchannel plate detector with an impedance matched anode in suspended substrate technology. *Review of Scientific Instruments.* **2001**, *72*(3), 1634.

[32] A. Riedo, M. Tulej, U. Rohner, P. Wurz. High-speed microstrip multi-anode multichannel plate detector system. *Review of Scientific Instruments.* **2017**, *88*(4), 045114.

[33] J.S. Becker. *Inorganic mass spectrometry : principles and applications.* Chichester, England ; Hoboken, NJ: John Wiley & Sons; 2007.

[34] L. Huber, E. Gnos, B. Hofmann, K.C. Welten, K. Nishizumi, M.W. Caffee, D.J. Hillegonds, I. Leya. The complex exposure history of the Jiddat al Harasis 073 L-chondrite shower. *Meteoritics & Planetary Science.* **2008**, *43*(10), 1691.